

Small fields measurements with radiochromic films

Antonio Gonzalez-Lopez, Juan-Antonio Vera-Sanchez¹, Jose-Domingo Lago-Martin

Hospital Universitario Virgen de la Arrixaca, Carretera Madrid-Cartagena, Murcia, ¹Servicio de Proteccion Radiologica y Fisica Medica, Hospital Sant Joan de Reus, Reus, Tarragona, Spain

Received on: 10-11-2014 Review completed on: 02-03-2015 Accepted on: 03-03-2015

ABSTRACT

The small fields in radiotherapy are widely used due to the development of techniques such as intensity-modulated radiotherapy and stereotactic radio surgery. The measurement of the dose distributions for small fields is a challenge. A perfect dosimeter should be independent of the radiation energy and the dose rate and should have a negligible volume effect. The radiochromic (RC) film characteristics fit well to these requirements. However, the response of RC films and their digitizing processes present a significant spatial inhomogeneity problem. The present work uses a method for two-dimensional (2D) measurement with RC films based on the reduction of the spatial inhomogeneity of both the film and the film digitizing process. By means of registering and averaging several measurements of the same field, the inhomogeneities are mostly canceled. Measurements of output factors (OFs), dose profiles (in-plane and cross-plane), and 2D dose distributions are presented. The field sizes investigated are $0.5 \times 0.5 \text{ cm}^2$, $0.7 \times 0.7 \text{ cm}^2$, $1 \times 1 \text{ cm}^2$, $2 \times 2 \text{ cm}^2$, $3 \times 3 \text{ cm}^2$, $6 \times 6 \text{ cm}^2$, and $10 \times 10 \text{ cm}^2$ for 6 and 15 MV photon beams. The OFs measured with the RC film are compared with the measurements carried out with a PinPoint ionization chamber (IC) and a Semiflex IC, while the measured transversal dose profiles were compared with Monte Carlo simulations. The results obtained for the OFs measurements show a good agreement with the values obtained from RC films and the PinPoint and Semiflex chambers when the field size is greater or equal than $2 \times 2 \text{ cm}^2$. These agreements give confidence on the accuracy of the method as well as on the results obtained for smaller fields. Also, good agreement was found between the measured profiles and the Monte Carlo calculated profiles for the field size of $1 \times 1 \text{ cm}^2$. We expect, therefore, that the presented method can be used to perform accurate measurements of small fields.

Key words: Film dosimetry, radiochromic films, small fields

Introduction

The increased use of radiotherapy techniques such as intensity-modulated radiotherapy and stereotactic radiosurgery has generalized the use of small fields. Also, some treatment units as the gammaknife or the cyberknife are based on the use of small fields. It is therefore important to have methods for the precise measurement of the dose for these kinds of fields.^[1-3]

The measurement of the dose distributions for small fields have beam geometries that are quite different from

the reference conditions stated in the dosimetry protocols. The radiation field does not produce constant dose volumes to encompass the volume of conventional detectors. Therefore, very small volume detectors are required to avoid volume averaging effects. This finite detector volume has been identified as the major reason for the measurement of low dose values in the non-constant dose regions.^[4] Moreover, the spectrum exhibits a dependence on the field size^[5] and the dose rate becomes smaller as the field size decreases, due to the loss of lateral electronic equilibrium.^[6] It is therefore necessary to use small volume dosimeters, with negligible energy and dose rate dependencies.^[7,8] However, it is hard to find dosimeters that meet all of these requirements.^[9]

Ionization chambers (ICs) have a small dependency on the energy of the radiation for the range of energies found in radiotherapy. However, in order to obtain a good signal to noise ratio, small sensitive volumes are not recommended. In this way the volume effect is not negligible for small field sizes, and the measurement in these non-constant dose regions is limited in accuracy.

Given the high spatial resolution of radiochromic (RC) films,^[10,11] the volume effect is not a concern in the dosimetry of radiotherapy beams. Its dependency on the

Address for correspondence:

Prof. Antonio Gonzalez-Lopez,
Hospital Universitario Virgen de la Arrixaca, Carretera
Madrid-Cartagena, 30120 El Palmar, Murcia, Spain.
E-mail: antonio.gonzalez7@carm.es

Access this article online	
Quick Response Code:	Website: www.jmp.org.in
	DOI: 10.4103/0971-6203.158667

dose rate and the beam energy is small.^[12,13] However, the response of RC films has a poor spatial homogeneity,^[12,14] and this may be their main drawback for dosimetric applications. Moreover, digitizing the films also introduces complex inhomogeneities. Lynch *et al.*,^[15] shows that important lateral inhomogeneities are introduced by a flatbed scanner, and these inhomogeneities are function of the optical density.

This work uses a method for small fields two-dimensional (2D) measurements with RC films based on the reduction of the spatial inhomogeneity of the film and the film reading. By means of averaging several measurements of a field, the heterogeneity is mostly canceled. In the same way, the calibration curve is obtained after averaging several measurements of each dose calibration value. The film pieces used for each dose value are selected from different locations of one sheet of film. In this way the uncertainty due to the spatial inhomogeneity of the film is strongly reduced. The positive characteristics of RC film are then exploited to measure output factors (OFs), dose profiles, and 2D dose distributions. The results obtained with the RC on OFs are compared with the measurements carried out with a PinPoint IC and a Semiflex IC, whereas the measured profiles are compared with profiles calculated by Monte Carlo methods.

Materials and Methods

The ICs used in this work were a 0.015 cm³ PinPoint thimble-type 31006 (PTW, Freiburg, Germany) and a 0.125 cm³ Semiflex thimble-type 31010. The RC film used was the EBT-2 film (International Specialty Products, Wayne, USA). After irradiation the films were digitized in a flatbed ScanMaker 9800XL (MicroTek, Hsinchu, Taiwan). The red channel of a 48 bits RGB digitization was then extracted and used as the digitizer reading. The resolution selected was 254 pixels per inch.

ICs and films were irradiated with 6 and 15 MV photon beams produced from a Varian 2100-DHX Linac (Varian Medical Systems). Films and ICs were placed in a PMMA phantom of size 30 × 30 × 20 cm³. The field sizes investigated were 0.5 × 0.5 cm², 0.7 × 0.7 cm², 1 × 1 cm², 2 × 2 cm², 3 × 3 cm², 6 × 6 cm², and 10 × 10 cm².

OFs for fields ranging from 0.5 × 0.5 cm² to 10 × 10 cm², and beam profiles and 2D dose distributions for fields of sizes 0.5 × 0.5 cm², 0.7 × 0.7 cm², and 1 × 1 cm² were measured with the secondary jaws delimiting the field size, at a depth of d_{\max} (1.5 cm for the 6 MV beams and 2.5 cm for the 15 MV beams) and 100 cm source-to-surface distance (SSD).

All measurement were performed with a gantry angle of 0° and a dose rate of 300 MU/min that correspond to 3 Gy/

min for a 10 × 10 cm² field, at d_{\max} and 100 cm SSD. The PinPoint and the Semiflex ICs were placed with their stems perpendicular to the beam axis. The maximum lengths of the sensitive volumes of both chambers are 5 and 6.5 mm, respectively; these lengths being equal or slightly larger than the smallest field lateral dimension, and larger than the constant dose region for some of the fields measured.

A number of segments of one sheet of film are used to carry out a calibration of the film response. Calibration segments of film are irradiated separately to known doses of 50, 170, 250, 320, 400, and 520 cGy. Then the segments are digitized and the readings obtained are used to fit a power function relating the digitizer reading to the dose. For each dose value 10 segments of film are read, and the readings are averaged before the curve fitting. The reading for each film calibration segment is obtained as the median of the pixel values in a ROI of 1.5 × 1.5 cm² in the center of the imaged segment.

A sheet of film is cut into segments of 2 × 2 cm², conforming a 2D array. The distribution of these segments is shown in Figure 1. For each dose value 10 segments of film are selected, so that each pair of segments is in different columns and rows of the array. The film segments are irradiated separately and 6 h after irradiation the films are arranged in the same way before being cut and read. In this way, after averaging all the pieces belonging to a dose value the effect of the spatial inhomogeneity is minimized.

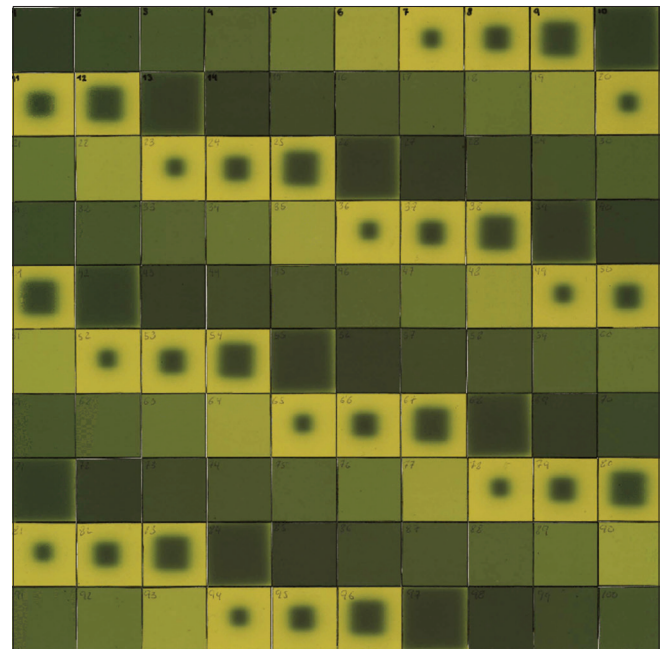


Figure 1: One of the films used for the measurement of the small fields. Six calibration fields (50, 170, 250, 320, 400, and 520 cGy) together with four fields of sizes 0.5 × 0.5 cm², 0.7 × 0.7 cm², 1 × 1 cm², and 2 × 2 cm² were used (these fields can be seen, for instance, in first row and columns 7, 8, 9 and 10 respectively). Each field was used to irradiate 10 film segments, and the readings of these 10 segments are averaged to minimize film inhomogeneities

For each small field ($0.5 \times 0.5 \text{ cm}^2$, $0.7 \times 0.7 \text{ cm}^2$, and $1 \times 1 \text{ cm}^2$), the images obtained after digitizing the pieces of films are registered. After averaging the registered images, the pixel values are converted to dose by applying the calibration curve. Then contour plots and transversal profiles are obtained.

Monte Carlo calculations of the $1 \times 1 \text{ cm}^2$ fields were carried out with the Penelope code^[16] and the spectra data for the 6 and 15 MV photon beams were taken from Daryoush and Rogers.^[17] A simplified simulation was carried out, aimed to simulate the effect of the collimator jaws in the penumbra of the small fields. The photon beam was modeled by a photon point source with the energy spectrum given by Daryoush and Rogers.^[17] The jaws and phantom materials and spatial dimensions were accurately modeled.

Results

Figure 2 shows the calibration curve relating the readings of the films and the irradiation doses. It is a power function $y = ax^b + c$, where y stands for the dose and x stands for the normalized pixel value. The adjusted R-square of the fit is 0.9998.

Figure 3 shows the reduction of uncertainty when applying the method of averaging of readings. This figure shows 100 curves (solid lines), randomly chosen from 100,000 possibilities. Each curve is obtained by fitting the readings of five pieces of film to the doses 520, 400, 320, 170, and 50 cGy. The curve obtained by fitting the averaged readings is also shown (bold and dashed line). Using this curve, the dose estimation for the films irradiated to 250 cGy (averaged readings) is 249.6 cGy. On the other hand, the standard deviation for the estimation based on one single piece of film for each dose value is 19 cGy.

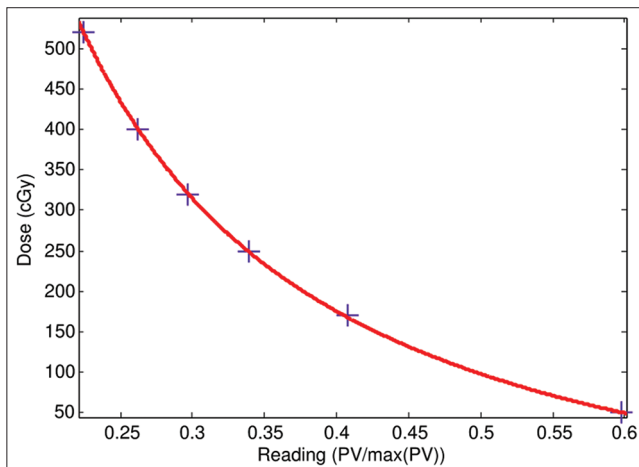


Figure 2: Calibration curve relating the reading of the films with the radiation doses. PV=Pixel value

Figure 4 shows contour plots of film measurements for the fields $0.5 \times 0.5 \text{ cm}^2$, $0.7 \times 0.7 \text{ cm}^2$, and $1 \times 1 \text{ cm}^2$. The isodoses shown are 80, 50, and 20% of the maximum dose for each of the 6 and 15 MV fields.

Figure 5 shows the transversal profiles measured with films for the fields of sizes $0.5 \times 0.5 \text{ cm}^2$, $0.7 \times 0.7 \text{ cm}^2$, and $1 \times 1 \text{ cm}^2$, and the energies 6 and 15 MV. The dashed lines correspond to the in-plane direction (gun-target direction) and the continuous lines correspond to the cross-plane direction (transversal to the in-plane). This figure shows the differences in the shape of the dose profiles for the in-plane and the cross-plane directions. In the Clinac 2100 the jaws delimiting the field in the in-plane are closer to the target, and this fact increases the penumbra in this direction.

Figures 6 and 7 show the transversal profiles for the field of size $1 \times 1 \text{ cm}^2$ and the energies 6 and 15 MV, respectively. The dashed lines correspond to the Monte Carlo calculations and the continuous lines correspond to the film measurements.

The measurements of the field sizes (determined as the full width half maximum) and penumbras 20–80% for the 6 and 15 MV beams are shown in Tables 1 and 2, respectively. The Monte Carlo calculations for the field of size $1 \times 1 \text{ cm}^2$ are also presented.

Figure 8 shows the measured OFs. The right side shows the measurements for the 6 MV energy beams, while the left side shows the measurements for the 15 MV beams, the error bars in the RC film measurements correspond to 1 standard deviation. In both cases a good agreement is found between both types of chambers (Semiflex and Pinpoint) and the RC films for field sizes of $2 \times 2 \text{ cm}^2$ or larger. However, as the field size becomes smaller, the differences appear.

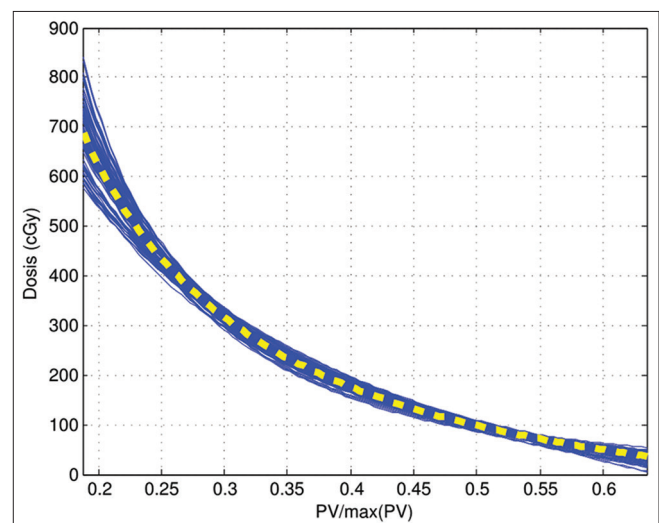


Figure 3: Calibration curves using one piece of film for dose values (solid lines) and averaging 10 film pieces for each dose value (dashed line)

Table 1: Field sizes (full width half maximum) and penumbras 20-80% in the in-plane (IP) and cross-plane (CP) directions for the fields shown in Figure 5a (6 MV beams)

Nominal field size	0.5×0.5 cm ²	0.7×0.7 cm ²	1×1 cm ²	
			RC film	Monte Carlo
Field size IP	4.5 mm	6.4 mm	9.4 mm	9.6 mm
Field size CP	4.7 mm	6.6 mm	9.8 mm	9.7 mm
Penumbra IP	2.0 mm	2.4 mm	2.6 mm	2.0 mm
Penumbra CP	1.6 mm	1.9 mm	2.0 mm	1.8 mm

For the 1×1 cm² field the Monte Carlo calculations are also presented.
RC=Radiochromic

Table 2: Field sizes (full width half maximum) and penumbras 20-80% in the in-plane (IP) and cross-plane (CP) directions for the fields shown in Figure 5b (15 MV beams)

Nominal field size	0.5×0.5 cm ²	0.7×0.7 cm ²	1×1 cm ²	
			RC film	Monte Carlo
Field size IP	5.0 mm	6.7 mm	9.5 mm	9.7 mm
Field size CP	4.8 mm	6.8 mm	9.9 mm	9.8 mm
Penumbra IP	2.5 mm	2.6 mm	3.0 mm	2.5 mm
Penumbra CP	2.1 mm	2.2 mm	2.5 mm	2.3 mm

For the 1×1 cm² field the Monte Carlo calculations are also presented.
RC=Radiochromic

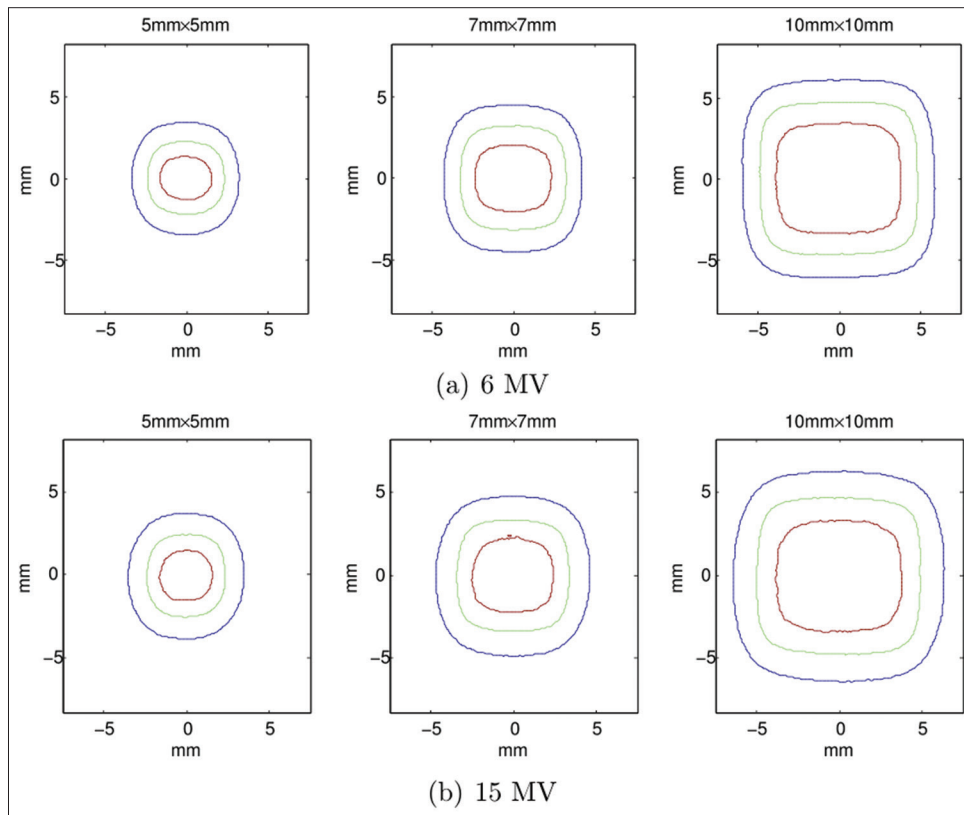


Figure 4: Contour plots of film measurements for the small fields. The isodose curves represent the 80, 50, and 10% of the maximum dose in each field

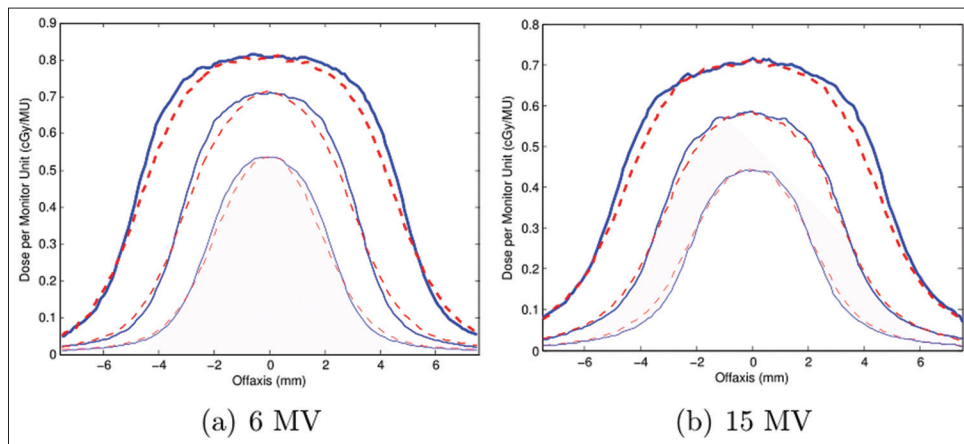


Figure 5: Transversal profiles measured with films for the 0.5 × 0.5 cm², 0.7 × 0.7 cm², and 1 × 1 cm² fields. The dotted lines correspond to the in-plane direction, while the solid lines correspond to the cross-plane direction

The measurement of the OF for the 6 MV field of size $1 \times 1 \text{ cm}^2$ with the Pinpoint and Semiflex chambers are 10 and 14% lower, respectively, than the OF measured

with the RC films. In the case of 15 MV, the corresponding differences are 10 and 18%, respectively. For the smallest fields the differences increase. For the $0.7 \times 0.7 \text{ cm}^2$, the

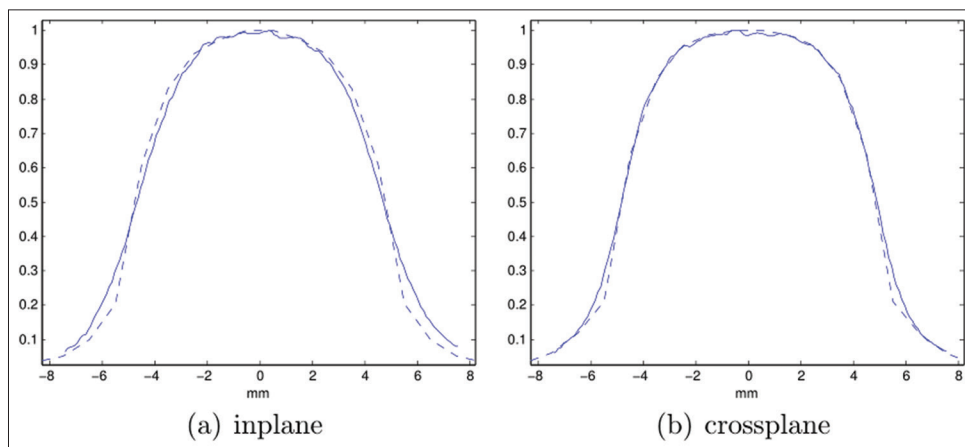


Figure 6: Transversal profiles for the $1 \times 1 \text{ cm}^2$ 6MV field. Film measurements (solid lines) and Monte Carlo calculations (dashed lines)

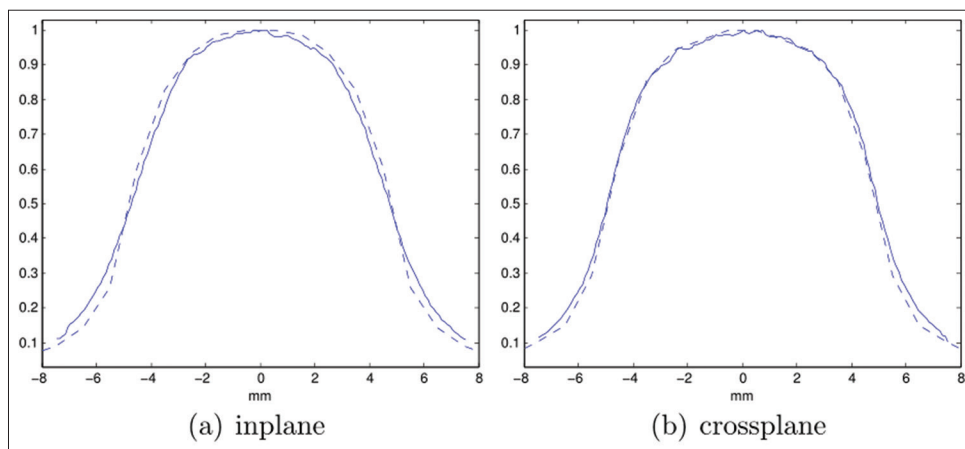


Figure 7: Transversal profiles for the $1 \times 1 \text{ cm}^2$ 15 MV field. Film measurements (solid lines) and Monte Carlo calculations (dashed lines)

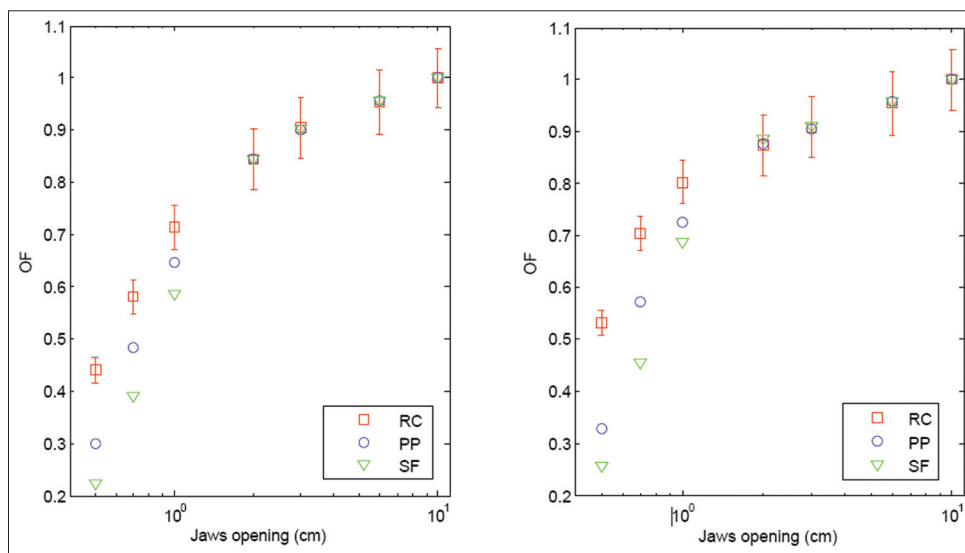


Figure 8: Output factors for the 6 and 15 MV beams. The field sizes range between $0.5 \times 0.5 \text{ cm}^2$ and $10 \times 10 \text{ cm}^2$. Error bars in the RC film measurements correspond to 1 standard deviation. RC = Radiochromic, PP = Pinpoint, SF = Semiflex

differences with the RC measurements are 19 and 35% for the 6 MV beams and 17 and 33% for the 15 MV, respectively. In the case of the 0.5×0.5 cm² field, the differences with the RC measurements are 38 and 52% for the 6 MV beams and 32 and 50% for the 15 MV beams, respectively.

Discussion and Conclusions

In this work a method to measure small radiotherapy fields by means of RC films has been presented. OFs, beam profiles, and 2D dose distributions are accurately measured, taking advantage of the dosimetric properties of the RC media. The small energy and dose rate dependencies shown by the RC films and their high spatial resolution are exploited for measuring small fields.

On the other hand, the method presented in this work shows how to deal with the main drawback of RC films: The spatial inhomogeneity of their response. This problem is even bigger when reading the film with a flatbed scanner. In this work, the inhomogeneity is mostly canceled by means of averaging the measurements over a number of segments taken from different parts of one sheet of film.

One advantage of using RC films is the possibility of accurately measuring the dose gradient regions. In-plane and cross-plane profiles are shown and the differences in penumbras are obtained, together with the full width at half maximum. Good agreement is found between the measured profiles and the Monte Carlo calculated profiles for the field size of 1×1 cm².

For the fields of size 1×1 cm² or smaller, the measurements of the OFs by means of the Pinpoint and Semiflex chambers is affected by the volume effect. The sensitive volume has a length of 5 mm for the Pinpoint chamber and of 6.5 mm for the Semiflex chamber. Those lengths are larger than the constant dose regions of the in-plane profiles [see Figure 5]. The measurement of the ICs averages the dose on these volumes, and therefore underestimates the dose in the central axis central axis (CAX).

The results obtained for the OFs' measurements show a good agreement between RC films and the PinPoint and Semiflex chambers when the field size is 2×2 cm². This agreement and the goodness of fit shown by the calibration curve gives confidence on the accuracy of the method.

The ICs are accurate when measuring fields of size 2×2 cm² or larger. For these fields, the OFs measured with RC films match the OFs measured with the ICs (being the differences smaller than 1.0%). It can be argued that, for large fields, the RC films' measurements are also accurate. Moreover, as reducing the field size is

not expected to change the accuracy of the RC films' measurements, as demonstrated through the extensive use of the RC films in the measurements of the OFs,^[18,19] the accuracy of the RC film measurements can be extrapolated to the small fields. The same can be said about the measurement depth; the material media, water instead of PMMA; the collimation system, multileaf collimator (MLC) instead of jaws; or even the irradiation unit. We expect, therefore, that the presented method can be used to perform accurate measurements of small fields in a wide range of situations.

References

1. Hardcastle N, Basavatia A, Bayliss A, Tom WA. High dose per fraction dosimetry of small fields with gafchromic EBT2 film. *Med Phys* 2011;38:4081-5.
2. García-Garduño OA, Lárraga-Gutiérrez JM, Rodríguez-Villafuerte M, Martínez-Dávalos A, Celis MA. Small photon beam measurements using radiochromic film and Monte Carlo simulations in a water phantom. *Radiother Oncol* 2010;96:250-3.
3. Hsu SM, Lee JH, Hsu FY, Lee HW, Hung SK, Liao YJ, *et al.* Dose measurements for gamma knife with radiophotoluminescent glass dosimeter and radiochromic film. *Radiat Prot Dosimetry* 2011;146:256-9.
4. Laub WU, Wong T. The volume effect of detectors in the dosimetry of small field sused in IMRT. *Med Phys* 2003;30:341-7.
5. Wu A, Zwicker RD, Kalend AM, Zheng Z. Comments on dose measurements for a narrow beam in radiosurgery. *Med Phys* 1993;20:777-9.
6. Das JJ, Ding GX, Ahnesjo A. Small fields: Nonequilibrium radiation dosimetry. *Med Phys* 2008;35:206-15.
7. Sanchez-Doblado F, Andreo P, Capote R, Leal A, Perucha M, Arrans R, *et al.* Ionization chamber dosimetry of small photon fields: A Monte Carlo study on stopping-power ratios for radiosurgery and IMRT beams. *Phys Med Biol* 2003;48:2081-99.
8. Westermark M, Arndt J, Nilson B, Brahme A. Comparative dosimetry in narrow high-energy photon beams. *Phys Med Biol* 2000;45:685-702.
9. Sauera O, Wilbert J. Measurement of output factors for small photon beams. *Med Phys* 2007;34:1983-8.
10. Fuss M, Sturtewagen E, De Wagter C, Georg D. Dosimetric characterization of GafChromic EBT film and its implication on film dosimetry quality assurance. *Phys Med Biol* 2007;52:4211-25.
11. Martisikova M, Ackermann B, Jkel O. Analysis of uncertainties in Gafchromic EBT film dosimetry of photon beams. *Phys Med Biol* 2008;53:7013-27.
12. Niroomand-Rad A, Blackwell CR, Coursey BM, Gall KP, Galvin JM, McLaughlin WL, *et al.* Radiochromic film dosimetry: Recommendations of AAPM Radiation Therapy Committee Task Group No. 55. American Association of Physicists in Medicine. *Med Phys* 1998;25:2093-115.
13. Arjomandy B, Taylor R, Anand A, Sahoo N, Gillin M, Prado K, *et al.* Energy dependence and dose response of Gafchromic EBT2 film over a wide range of photon, electron, and proton beam energies. *Med Phys* 2010;37:1942-7.
14. Hartmann B, Martisikova M, Jakel O. Homogeneity of Gafchromic EBT2 film. *Med Phys* 2010;37:1753-6.
15. Lynch BD, Kozelka J, Ranade MK, Li JG, Simon WE, Dempsey JF. Important considerations for radiochromic film dosimetry with film flatbed CCD scanners and EBT GAFCHROMIC film. *Med Phys* 2006;33:4551-6.
16. Salvat F, Fernandez-Varea JM, Sempau J. A code system for Monte

- Carlosimulation of electron and photon transport. Barcelona. NEA Workshop Proceedings; 2008.
17. Sheikh-Bagheri D, Rogers DW. Monte Carlo calculation of nine megavoltage photon beam spectra using the BEAM code. *Med Phys* 2002;29:391-402.
 18. Wilcox EE, Daskalov GM. Evaluation of GAFCHROMIC EBT film for Cyberknife dosimetry. *Med Phys* 2007;34:1967-74.
 19. Sharma SD, Kumar S, Dagaonkar SS, Bisht G, Dayanand S, Devi R,

et al. Dosimetric comparison of linear accelerator-based stereotactic radiosurgery systems. *J Med Phys* 2007;32:18-23.

How to cite this article: Gonzalez-Lopez A, Vera-Sanchez JA, Lago-Martin JD. Small fields measurements with radiochromic films. *J Med Phys* 2015;40:61-7.

Source of Support: Nil, **Conflict of Interest:** None declared.